PHYSICAL REVIEW D **92,** 014014 (2015)

Testing the consistency of the $\omega\pi$ transition form factor with unitarity and analyticity

I. Caprini

Horia Hulubei National Institute for Physics and Nuclear Engineering, P.O.B. MG-6, 077125 Bucharest-Magurele, Romania

(Received 20 May 2015; published 10 July 2015)

We perform a dispersive analysis of the $\omega\pi$ electromagnetic transition form factor, using as input the discontinuity provided by unitarity below the $\omega\pi$ threshold and including for the first time experimental data on the modulus measured from $e^+e^- \to \omega\pi^0$ at higher energies. The input leads to stringent parametrization-free constraints on the modulus of the form factor below the $\omega\pi$ threshold, which are in disagreement with some experimental values measured from $\omega \to \pi^0\gamma^*$ decay. We discuss the dependence on the input parameters in the unitarity relation, using for illustration an N/D formalism for the P partial wave of the scattering process $\omega\pi \to \pi\pi$, improved by a simple prescription which simulates the rescattering in the crossed channels. Our results confirm the existence of a conflict between experimental data and theoretical calculations of the $\omega\pi$ form factor in the region around 0.6 GeV and bring further arguments in support of renewed experimental efforts to measure more precisely the $\omega \to \pi^0\gamma^*$ decay.

DOI: 10.1103/PhysRevD.92.014014 PACS numbers: 13.40.Gp, 11.55.Fv, 13.25.Jx

I. INTRODUCTION

The transition form factors of light mesons play an important role in low energy precision tests of QCD [1]. In particular, they enter as contributions to hadronic light-by-light scattering calculations [2], which are crucial for a more accurate theoretical determination of the standard model prediction for the muon's anomalous magnetic moment (for recent reviews see [3,4]).

The case of the $\omega\pi$ electromagnetic form factor is particularly interesting as there are some discrepancies between the theoretical calculations and the experimental data from the decay $\omega \to \pi^0\gamma^*$ reported in [5–7]. This form factor was described by the vector meson dominance model and by a chiral Lagrangian approach in [8,9]. Calculations based on a standard dispersion relation were performed a long time ago in [10] and recently in [11,12]. The discontinuity of the form factor required in the Cauchy integral can be expressed in terms of known observables by using unitarity. The two-pion contribution to the unitarity sum gives the discontinuity in terms of the P partial wave of the amplitude of the process $\omega\pi \to \pi\pi$, itself calculated in the dispersion theory [10,12,13], and the pion electromagnetic form factor, a quantity which is known with very good precision. However, the two-pion approximation is valid only in a region which extends to a good approximation up to the $\omega\pi$ threshold, $t_+ = (m_\omega + m_\pi)^2$. Due to the lack of information on the discontinuity above this threshold, various assumptions were adopted for the evaluation of the dispersion integral, either by applying the two-pion approximation also at higher energies [10,11], or by expanding the dispersion integral in powers of a suitable variable [12].

A study performed recently in [14] used as input above the $\omega\pi$ threshold, instead of the discontinuity, a model-independent integral condition on the modulus squared of the $\omega\pi$ form factor. The condition was obtained by using an approach proposed originally by Okubo [15], which has come to be known as the method of unitarity bounds (a recent review of this approach is presented in [16]). It exploits unitarity and the positivity of the spectral function of a suitable current-current correlator, calculated by operator product expansion in the Euclidean region. In the particular case of the $\omega\pi$ form factor, the method, adapted to the specific input conditions available, led eventually to a functional optimization problem of a type considered for the first time in [17,18]. The solution of the problem yields upper and lower bounds on the modulus of the $\omega\pi$ form factor in the region $4m_\pi^2 \le t < t_+$ [14]. A specific feature encountered in this case is that the discontinuity of the form factor across the cut is not purely imaginary. As a consequence, the form factor is not a real analytic function, as happens in familiar cases like the pion vector form factor. Therefore, in [14] the formalism of bounds was extended to functions which are not real analytic. Although not very stringent, the bounds derived in [14] are in disagreement with the experimental data on the modulus of the form factor in the region around 0.6 GeV, measured from the decay $\omega \to \pi^0\gamma^*$, confirming thus the conclusion of the analysis [11] based on standard dispersion theory.

It is important to note that the dispersive analyses performed so far did not include experimental data on the form factor available in the scattering region, above the $\omega\pi$ threshold. Measurements of the modulus from the reaction $e^+e^- \to \omega\pi^0$ are reported in [19–25] [a set of such data is shown in Fig. 1, where we show for completeness also the modulus measured in the decay region $t < t_-$,

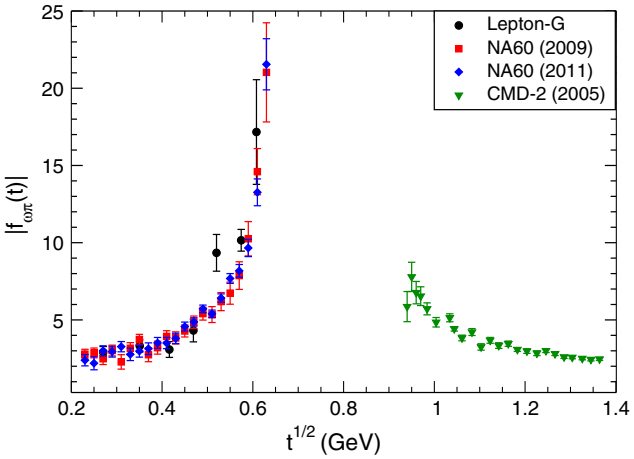

FIG. 1 (color online). Modulus of the $\omega\pi$ form factor measured from $\omega \to \pi^0\gamma^*$ decay by Lepton-G [5], NA60 (2009) [6] and NA60 (2011) [7], and from $e^+e^- \to \omega\pi^0$ by CMD-2 (2005) [22].

$t_- = (m_\omega - m_\pi)^2$]. In the present paper we consider the problem of including this information in the dispersive formalism. Specifically, we perform an analysis of the form factor using as input the discontinuity for $t < t_+$, calculated in a theoretical model based on unitarity, and experimental information on the modulus for $t > t_+$. Even though the modulus is not known at all energies, we can implement the information in a conservative way, as a condition on a weighted integral of the modulus squared from t_+ to infinity. This leads to a mathematical problem similar to that encountered and solved in [14]. The result is expressed in the form of explicit upper and lower bounds on the modulus of the $\omega\pi$ form factor below t_+, calculable in terms of the discontinuity below t_+ and the modulus above t_+. The formalism provides therefore a consistency test for the experimental data on the $\omega\pi$ electromagnetic form factor, which exploits analyticity and unitarity in a parametrization-free way.

The theoretical input of the test consists from the unitarity relation giving the discontinuity of the form factor, which involves the amplitude of the $\pi\omega \to \pi\pi$ scattering. It is of interest to study the influence of the possible uncertainties in this part of the input. The full calculation involves the solution of integral equations known as Khuri-Treiman equations [26]. The amplitudes reported in [12,13] are obtained by solving numerically these integral equations. Therefore, the dependence on the free parameters used in the calculations is not very transparent. The older treatment performed in [10], based on N/D formalism, has the advantage of providing explicit expressions depending on physical parameters. However, that treatment is not entirely satisfactory, as it does not account for the rescatterings between all the final pions in the kinematical region where the decay $\omega \to \pi\pi\pi$ is allowed. It is worthwhile trying to cure the shortcomings of this approach. In this paper we consider an improved N/D treatment, obtained by applying to [10] a prescription proposed in [27] for including finite-width effects in the resonances exchanged in the crossed channels. The improved model captures the essential features of the full solution, still preserving the explicit dependence on the input parameters. This has enabled us to investigate the influence of the uncertainties affecting the theoretical input of the consistency test.

The paper is organized as follows. In the next section we review the basic definitions and show how the input information on the form factor can be expressed as an extremal problem for analytic functions. In Sec. III we review the main steps of the proof and write down the solution of the extremal problem obtained in Ref. [14]. The results are presented in Sec. IV, where we discuss also their dependence on the parameters of the input. Section V contains our conclusions. The paper has an Appendix where we describe briefly the N/D model of [10] and an improved version based on a prescription suggested in [27].

II. INPUT IN THE CONSISTENCY TEST

We begin with a brief description of the form factor and the constraints that it satisfies. We use the conventions of [11], where the form factor $f_{\omega\pi}(t)$ is defined from the matrix element

$$\langle \omega(p_a,\lambda)\pi^0(p_b)|j_\mu(0)|0\rangle = i\epsilon_{\mu\tau\rho\sigma}\epsilon^{\tau *}(p_a,\lambda)p_b^\rho q^\sigma f_{\omega\pi}(t), \tag{1}$$

where j_μ is the isovector part of the electromagnetic current, λ denotes the ω polarization, $q = p_a + p_b$ and $t = q^2$. In the convention adopted here[1] the form factor $f_{\omega\pi}(t)$ has dimension of GeV^{-1}.

Unitarity implies that $f_{\omega\pi}(t)$ has a cut along the real axis for $t \geq 4m_\pi^2$. Keeping the two-pion contribution in the unitarity sum, the discontinuity of $f_{\omega\pi}(t)$ across the cut is written as

$$\mathrm{disc} f_{\omega\pi}(t) = \frac{iq(t)^3}{6\pi\sqrt{t}} F_\pi^*(t) f_1(t)\theta(t-4m_\pi^2), \qquad t \leq t_+, \tag{2}$$

where $q(t) = \sqrt{t/4 - m_\pi^2}$ is the center of mass momentum of the pion pair, $F_\pi(t)$ is the pion electromagnetic form factor and $f_1(t)$ the P partial-wave amplitude of the scattering

[1]The dimensionless form factor $F_{\pi\omega\gamma}(t)$ defined in [10] is related to the definition adopted here by $F_{\pi\omega\gamma}(t) = m_\omega f_{\omega\pi}(t)$. The form factor $F_{\pi\omega}(t)$ defined in [27] is dimensionless, normalized as $F_{\pi\omega}(0) = 1$ and is related to our definition by $f_{\omega\pi}(t) = 2\sqrt{2\tilde{C}_\omega} F_{\pi\omega}(t)$, where $\tilde{C}_\omega$ is defined in Eq. (35) of [27] in terms of the total width $\Gamma_{\omega\to\pi^0\gamma}$.

$$\omega(p_a,\lambda)\pi^0(p_b)\to\pi^+(q_1)\pi^-(q_2). \tag{3}$$

The scattering process is physical for $t\geq t_+$. In the region $4m_\pi^2<t<t_-$, where the decay $\omega\to\pi^+\pi^-\pi^0$ is allowed, $f_1(t)$ is the P-wave projection of the decay amplitude, while the region $t_-<t<t_+$ is unphysical.

The amplitude $f_1(t)$ was calculated in [10] in the frame of N/D formalism, with the left-hand cut described by poles in the crossed channels due to the exchange of the ρ meson assumed to be stable. In this model, the phase of $f_1(t)$ coincides with the $\pi\pi$ P-wave phase shift and exactly compensates in the discontinuity (2) the phase of $F_\pi^*(t)$, related also to the $\pi\pi$ P wave phase shift δ_1^1 by Watson theorem [28]. Therefore, the form factor $f_{\omega\pi}(t)$ calculated in [10] is a real analytic function.[2]

In the more complete calculation [11–13] based on Khuri-Treiman formalism [26], the amplitude $f_1(t)$ is obtained by numerically solving a set of integral equations. Due to the rescattering between the final pions in the decay region $4m_\pi^2<t<t_-$, the phase of $f_1(t)$ does not coincide with the $\pi\pi$ P-wave phase shift, as one would naively expect from Watson theorem. Therefore, the phases of the two factors in (2) do not compensate each other, and the discontinuity (2) is not purely imaginary [11,12]. In other words, the $\omega\pi$ form factor is not a real analytic function, which is true also in the case of other transition form factors [27].

The expression (2) is valid only in the region $4m_\pi^2\leq t<t_+$, since above the $\omega\pi$ threshold other intermediate states, besides the two-pion states, contribute to the unitarity sum. So, strictly speaking the discontinuity of $f_{\omega\pi}(t)$ is not available for $t>t_+$. On the other hand, the modulus of $f_{\omega\pi}(t)$ can be extracted from experimental data on the $e^+e^-\to\omega\pi^0$ process, measured in [19–25]. The connection between the cross section and the modulus [10,27] is, in our convention,

$$\sigma_{e^+e^-\to\omega\pi^0}(t)=\frac{4\pi\alpha^2}{3}\frac{p(t)^3}{t^{3/2}}|f_{\omega\pi}(t)|^2, \tag{4}$$

where $p(t)=\sqrt{(t-t_-)(t-t_+)/4t}$ is the center of mass momentum of the $\omega\pi$ pair in the rest system of the virtual photon and we recall that $t_\pm=(m_\omega\pm m_\pi)^2$.

Using the experimental data on the modulus and the asymptotic decrease like $1/t$ predicted by perturbative QCD scaling [29], it is possible to obtain a reasonable estimate of a weighted integral over the modulus squared from t_+ to infinity. Thus, we adopt an L^2-norm condition of the form

$$\frac{1}{\pi}\int_{t_+}^{\infty}|f_{\omega\pi}(t)|^2w(t)dt=I, \tag{5}$$

where $w(t)$ is a suitable weight, chosen such as to allow a precise evaluation of the quantity I. A similar way of including experimental information on the modulus at higher energies was adopted in the recent investigations [30,31] of the pion electromagnetic form factor.

Of course, the condition (5) is weaker than the information provided at each t by (4). However, measurements of the cross section are available only at a finite number of discrete values of energy, which are not sufficient for a parametrization-free approach like the one considered in this paper. Moreover, the modulus is not known at higher energies. In the present analysis we have considered weights of the simple form

$$w(t)=\frac{1}{t^c}, \tag{6}$$

where the value of $c>0$ is taken such as to suppress the contribution to the integral of the intermediate and high energies, where the form factor is not known. In practice we evaluated the quantity I using an interpolation of the data on modulus from [22] shown in Fig. 1 from $t_+=0.84\ \mathrm{GeV}^2$ up to $t=1.86\ \mathrm{GeV}^2$, continued in a smooth way with a modulus $|f_{\omega\pi}(t)|$ decreasing like $1/t$. As will be clear in the next section, for a fixed weight the results of the formalism depend monotonically on the numerical value of I, in the sense that a larger I gives weaker results. Therefore, for a conservative estimate, we have used as input in the data region the central values from [22] enlarged by their quoted errors. For $c=2$ this leads to

$$I=4.63\ \mathrm{GeV}^{-4}, \tag{7}$$

where the region above $1.86\ \mathrm{GeV}^2$ contributes to the integral with about 8%.

Finally, we use as input the value of $|f_{\omega\pi}(0)|$, known experimentally from the $\omega\to\pi^0\gamma$ decay rate. The updated value is [32]

$$|f_{\omega\pi}(0)|=(2.30\pm0.04)\ \mathrm{GeV}^{-1}. \tag{8}$$

The aim of the present paper is to check the consistency of the data shown in Fig. 1 with unitarity and analyticity. To this end we shall compare the experimental data below t_- with the allowed ranges of the modulus $|f_{\omega\pi}(t)|$ which follow from analyticity, unitarity and the data available above t_+. Mathematically, the problem amounts to deriving upper and lower bounds on $|f_{\omega\pi}(t)|$ for $t<t_+$, upon the class of functions $f_{\omega\pi}(t)$ analytic in the t-plane cut for $t\geq4m_\pi^2$, which satisfy the following conditions: (i) their discontinuity is given by (2) in the region $t<t_+$, (ii) they satisfy the constraint (5), and (iii) they satisfy the condition

[2]A function $F(t)$ analytic in the t-plane cut for $t\geq4m_\pi^2$ is of real type if it satisfies the condition $F(t^*)=(F(t))^*$. In particular, this implies that the function is real on the real axis for $t<4m_\pi^2$, and its discontinuity across the cut can be written as disc $F(t)\equiv F(t+i\epsilon)-F(t-i\epsilon)=2i\mathrm{Im}F(t+i\epsilon)$.

(8). The solution of this mathematical problem will be given in the next section.

III. SOLUTION OF THE EXTREMAL PROBLEM

An extremal problem of the type mentioned above was solved for the first time in [17,18] on the class of real analytic functions. The generalization to functions which are not real analytic was investigated in detail in [14]. We do not repeat the whole proof here, but only outline the main steps and write down the solution.

The first step is to map the t plane cut along $t \geq t_+$ onto the unit disk $|z| \leq 1$ in the $z \equiv \tilde{z}(t)$ plane. We have adopted the conformal mapping

$$\tilde{z}(t) = \frac{1 - \sqrt{1 - t/t_+}}{1 + \sqrt{1 - t/t_+}}, \tag{9}$$

which brings the origin of the t-plane to the origin of the z plane, $\tilde{z}(0) = 0$. In the z-plane the elastic region $4m_\pi^2 \leq t < t_+$ becomes the segment $x_\pi \leq x < 1$ of the real axis, where $x_\pi = \tilde{z}(4m_\pi^2) > 0$, and the upper (lower) edges of the cut $t > t_+$ become the upper (lower) semicircles.[3]

Further, we construct a so-called outer function [33], i.e., a function analytic and without zeros in $|z| < 1$, its modulus on $|z| = 1$ being equal to $\sqrt{w(\tilde{t}(z))|d\tilde{t}(z)/dz|}$, where $w(t)$ is the weight appearing in (5) and $\tilde{t}(z)$ is the inverse of the function $\tilde{z}(t)$ defined in (9). The general expression of the outer functions is given in [33] (see also the review [16]). For weights $w(t)$ of the form (6), we obtain for the outer function, denoted as $C(z)$, the exact analytic expression [16]

$$C(z) = (2\sqrt{t_+})^{1-c}(1-z)^{1/2}(1+z)^{c-3/2}. \tag{10}$$

From this expression it follows that $C(x)$ is real and positive on the segment $-1 < x < 1$, which corresponds in the t-plane to the semiaxis $t < t_+$.

If we introduce now a new function $h(z)$ by

$$h(z) = C(z) f_{\omega\pi}(\tilde{t}(z)), \tag{11}$$

the condition (5) takes the simple form

$$\frac{1}{2\pi}\int_0^{2\pi} d\theta |h(e^{i\theta})|^2 = I. \tag{12}$$

The function $h(z)$ is analytic in $|z| < 1$ except for a cut along the segment $(x_\pi, 1)$, where its discontinuity is

$$\mathrm{disc}\, h(x) \equiv \Delta(x) = C(x)\mathrm{disc} f_{\omega\pi}(\tilde{t}(x)). \tag{13}$$

By expressing $h(z)$ as

$$h(z) = \frac{1}{2\pi i}\int_{x_\pi}^1 \frac{\Delta(x)}{x - z} dx + g(z), \tag{14}$$

the new function $g(z)$ is analytic in $|z| < 1$, as its discontinuity across the cut vanishes:

$$\mathrm{disc}\, g(x) = 0, \qquad x \in (x_\pi, 1). \tag{15}$$

Since we consider in general form factors that are not real analytic, the function $g(z)$ is analytic, but its values on the real axis may be complex.

We now express the available information on the form factor as a number of constraints on the function g. By inserting (14) in (12) we obtain the condition

$$\frac{1}{2\pi}\int_0^{2\pi} d\theta \left| \frac{1}{2\pi i}\int_{x_\pi}^1 \frac{\Delta(x)}{x - e^{i\theta}} dx + g(e^{i\theta}) \right|^2 = I, \tag{16}$$

and using (11) and (14) we write $g(0)$ as[4]

$$g(0) = f_{\omega\pi}(0)C(0) - \frac{1}{2\pi i}\int_{x_\pi}^1 \frac{\Delta(x)}{x} dx. \tag{17}$$

The problem is to find the maximal allowed range of $|g(z_1)|$ at an arbitrary given point $z_1 = \tilde{z}(t_1)$ in the interval $(x_\pi, 1)$, for functions $g(z)$ analytic in $|z| < 1$ and subject both to the boundary condition (16) and the additional constraint (17).

It is useful to denote

$$g(z_1) = \xi, \tag{18}$$

where ξ is an unknown parameter. Then one can prove (see for instance [18]) that the allowed range of ξ is described by the inequality[5]

$$\mu_2^2(\xi) \leq I, \tag{19}$$

where $\mu_2^2(\xi)$ is the solution of the functional minimization problem

$$\mu_2^2(\xi) = \min_{g \in \mathcal{G}_\xi} \frac{1}{2\pi}\int_0^{2\pi} d\theta \left| \frac{1}{2\pi i}\int_{x_\pi}^1 \frac{\Delta(x)}{x - e^{i\theta}} dx + g(e^{i\theta}) \right|^2, \tag{20}$$

upon the class $\mathcal{G}_\xi$ of functions $g(z)$ analytic in $|z| < 1$, which satisfy the constraint (17) and the additional condition (18) for a given ξ.

The constrained minimum norm problem (20) was solved in [14] by the technique of Lagrange multipliers, leading to a solution written in compact form:

[3] Other mappings are obtained by changing the point that is mapped onto the origin of the z-plane. It can be shown [16] that the results do not depend on the choice of the conformal mapping.

[4] Note that the expression of $g(0)$ given in Eq. (24) of Ref. [14] contains a misprint (which actually did not affect the results, since the calculations were performed with the correct expression).

[5] This shows that the results remain the same if (5) is replaced by an inequality involving a quantity that majorizes I.

$$\mu_2^2(\xi) = \frac{1}{4\pi^2}\int_{x_\pi}^1\int_{x_\pi}^1 \frac{\Delta(x)\Delta^*(y)}{1-xy}\,dxdy + |g(0)|^2 + \frac{1-z_1^2}{z_1^2}|\xi - g(0)|^2. \tag{21}$$

By inserting (21) in (19) we obtain upper and lower bounds on the parameter ξ. Expressed in terms of the form factor $f_{\omega\pi}(t)$ by using Eqs. (11) and (14), they lead to the inequalities [14]:

$$|f_{\omega\pi}(t)| \le \frac{\left|g(0) + \frac{1}{2\pi i}\int_{x_\pi}^1 \frac{\Delta(x)}{x-\tilde z(t)}\,dx\right| + \frac{\tilde z(t) I'}{\sqrt{1-\tilde z(t)^2}}}{C(\tilde z(t))},$$
$$|f_{\omega\pi}(t)| \ge \frac{\left|g(0) + \frac{1}{2\pi i}\int_{x_\pi}^1 \frac{\Delta(x)}{x-\tilde z(t)}\,dx\right| - \frac{\tilde z(t) I'}{\sqrt{1-\tilde z(t)^2}}}{C(\tilde z(t))}, \tag{22}$$

where $\tilde z(t) \in (x_\pi, 1)$ is the image of the point t in the z-plane, and

$$I' = \left[I - \frac{1}{4\pi^2}\int_{x_\pi}^1\int_{x_\pi}^1 \frac{\Delta(x)\Delta^*(y)}{1-xy}\,dxdy - |g(0)|^2\right]^{1/2}. \tag{23}$$

We recall that $C(\tilde z(t)) > 0$ for $t < t_+$, which justifies its appearance outside the modulus sign in the denominator of (22).

The upper and lower bounds (22) are calculable in terms of the input defined in the previous section. They determine an allowed interval for the modulus $|f_{\omega\pi}(t)|$ at every $t < t_+$. From (22) it follows that, for a fixed weight $w(t)$ in the L^2-norm constraint (5), the bounds depend monotonically on the value of I: smaller values of I lead to narrower allowed intervals for $|f_{\omega\pi}(t)|$ at $t < t_+$. We already took into account this property for a conservative estimate of I, as discussed in the previous section.

It is useful to remark also that, since the last term in (21) is positive, from (19) and (21) we can write down the inequality

$$\frac{1}{4\pi^2}\int_{x_\pi}^1\int_{x_\pi}^1 \frac{\Delta(x)\Delta^*(y)}{1-xy}\,dxdy + |g(0)|^2 \le I, \tag{24}$$

where $g(0)$ is defined in (17) and $\Delta(x)$ is (13). The inequality (24) involves only input quantities and represents a necessary condition that must be satisfied by them. If it is violated, the input is not consistent with analyticity and unitarity.

IV. RESULTS

We have investigated several suitable weights of the form (6) and checked that they lead to similar results. The calculations reported below were done with the choice $c = 2$, which ensures a good suppression of the high energy part of the integral.

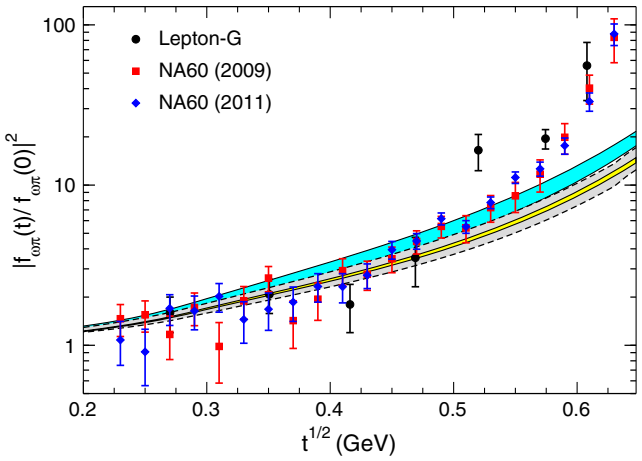

FIG. 2 (color online). Upper and lower bounds compared with experimental data on $|f_{\omega\pi}(t)/f_{\omega\pi}(0)|^2$. Cyan band: bounds calculated using in the discontinuity (2) the partial wave amplitude $f_1(t)$ from [10]. Grey band: bounds calculated using in the discontinuity (2) the amplitude $f_1(t)$ from [11]. The yellow band is the result of the dispersive calculation performed in [11]. The data are from Lepton-G [5], NA60 (2009) [6] and NA60 (2011) [7].

As already mentioned, we have taken the discontinuity (2) of the $\omega\pi$ form factor in the range $(4m_\pi^2, t_+)$ from the recent dispersive treatment reported in [11] and from the older work [10]. The pion vector form factor $F_\pi(t)$ entering (2) has been calculated in [11] from an Omnès representation [34] using as input the pion-pion phase shift $\delta_1^1(t)$ obtained from Roy equations in [35,36]. In [10], the pion form factor was described by a Gounaris-Sakurai representation given in Eqs. (A14)–(A16) of the Appendix. The differences between the two representations of the pion form factor are very small and have a negligible influence on the results. On the other hand, Refs. [10] and [11] differ substantially in the dispersive calculation of the partial wave $f_1(t)$ required also as input in (2).

In Fig. 2 we show the allowed range of the modulus squared (normalized to its value at $t = 0$), determined by the upper and lower bounds calculated in this paper, in the part of the elastic region accessible experimentally in $\omega \to \pi^0\mu^+\mu^-$ decay. The curves have been obtained using the expressions (22), which contain only known input quantities. For the discontinuity $\Delta(x)$ we have used the numerical solution[6] obtained in Ref. [11], and the model [10], presented in the Appendix. The results shown in Fig. 2 were obtained by varying the input value at $t = 0$ inside the error bar given in (8) and taking the weakest bounds, i.e., the largest allowed bands at each energy. For comparison, we also show the result of the dispersive

[6]I am grateful to Bastian Kubis for this input.

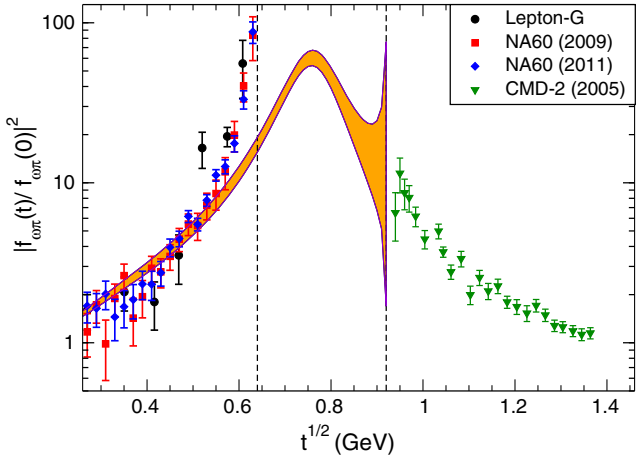

FIG. 3 (color online). Orange band: bounds on $|f_{\omega\pi}(t)/f_{\omega\pi}(0)|^2$ in the whole region $t < t_+$, obtained with the improved N/D model for the partial wave $f_1(t)$. The data are from Lepton-G [5], NA60 (2009) [6], NA60 (2011) [7] and CMD-2 (2005) [22].

calculation performed in [11], and several experimental data from [5–7].

With the input discontinuity from [11], the allowed band is consistent with the dispersion relation calculation performed in that work. The allowed band obtained with the partial wave $f_1(t)$ from [10] is shifted upwards and the two bands do not overlap. For both inputs the upper bounds shown in Fig. 2 are significantly lower than the data from [5–7] in the region around 0.6 GeV.

We mention that the upper and lower bounds shown in Fig. 2 are much more stringent than the upper and lower bounds obtained in [14] with the same input on the discontinuity (2), but with a model-independent condition on the modulus above the $\omega\pi$ threshold.[7]

It is of interest to understand the origin of the difference between the two predictions shown in Fig. 2. To this end, we have calculated the bounds using also the improved version of the N/D model for the partial wave $f_1(t)$, which includes the effect of rescattering in the crossed channels as discussed in the Appendix. The improvement has the effect of shifting the bounds downwards, towards the band calculated with the input amplitude $f_1(t)$ from [11,13], but the shift is small, of a few percents. For illustration we present in Fig. 3 the bounds calculated with the improved N/D model for $f_1(t)$ in the whole range $t < t_+$.

As follows from Eqs. (A5) and (A19) of the Appendix, the N/D model contains as input the dimensionless coupling constants $g_{\rho\pi\pi}$ and $g_{\omega\rho\pi}$. The results presented in Figs. 2 and 3 have been obtained using the values from [10]

$$g_{\rho\pi\pi} = 5.96, \qquad g_{\omega\rho\pi} = 13.42. \tag{25}$$

The quantity $g_{\rho\pi\pi}$ has not changed significantly over the past 40 years, the value (25) being fully consistent with the PDG-2014 width Γ_ρ, quoted below Eq. (A16). On the other hand, the coupling $g_{\omega\rho\pi}$ is still not very well known. We note that the dimensionless constant $g_{\omega\rho\pi}$ used here is related to the similar parameter used in [22,27], which we denote as $\tilde{g}_{\omega\rho\pi}$ to avoid confusion, by $g_{\omega\rho\pi} = m_\omega \tilde{g}_{\omega\rho\pi}$. The values $\tilde{g}_{\omega\rho\pi} = (13.8 \pm 0.3)$ GeV^{-1} obtained in [27] from a global fit of the $\omega\pi$ form factor, and $\tilde{g}_{\omega\rho\pi} = (16.7 \pm 0.4 \pm 0.6)$ GeV^{-1} derived in [22] from a fit of the cross section of $e^+e^- \to \omega\pi^0$, correspond in our notation to the values $g_{\omega\rho\pi} = 10.80 \pm 0.23$ and $g_{\omega\rho\pi} = 13.07 \pm 0.31 \pm 0.47$, respectively. We note that, while the above references consider parametrizations of the $\omega\pi$ form factor, in the present analysis the coupling $g_{\omega\rho\pi}$ is an input parameter in the model of the partial-wave amplitude $f_1(t)$.

One might ask whether a suitable choice of the parameter $g_{\omega\rho\pi}$ can reduce the conflict between the calculated bounds and the experimental data. We have investigated this question using the improved N/D model discussed in the Appendix. We remark first that for values $g_{\omega\rho\pi} > 15.5$ the inequality (24), which expresses a consistency condition on the input, is violated. Therefore, values of $g_{\omega\rho\pi}$ larger than 15.5 are not allowed, being inconsistent with the other input quantities [the data above t_+ and the value (8) at $t = 0$] and the general properties of analyticity and unitarity.

In Fig. 4 we show the allowed bands calculated with three choices of the couplings $g_{\omega\rho\pi}$: the value (25), a smaller

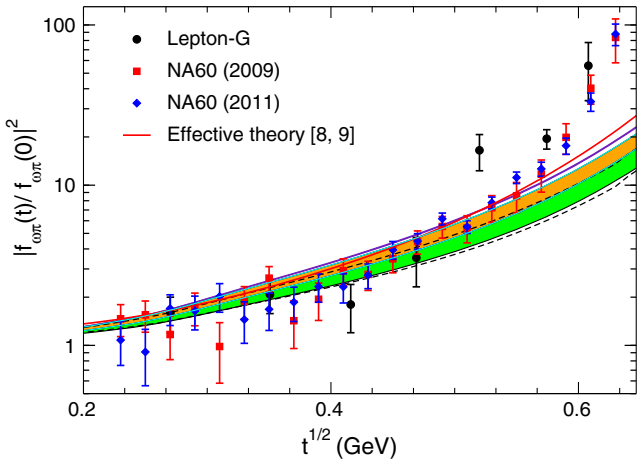

FIG. 4 (color online). Upper and lower bounds on $|f_{\omega\pi}(t)/f_{\omega\pi}(0)|^2$ calculated using the improved N/D model for $f_1(t)$, with $g_{\omega\rho\pi} = 11.5$ (green band) $g_{\omega\rho\pi} = 13.42$ (orange band) and $g_{\omega\rho\pi} = 15.5$ (indigo line). The dashed lines are the bounds calculated with the discontinuity (2) from [11]. The red line is the form factor calculated in [8,9] with a low-energy effective theory.

[7]For instance, the allowed range of the ratio $|f_{\omega\pi}(t)/f_{\omega\pi}(0)|^2$ at 0.64 GeV obtained in [14] with input discontinuity from [11] is (1.6, 36.8), while the range predicted in this paper with the same discontinuity is (11.3, 15.7).

value, $g_{\omega\rho\pi} = 11.5$, and the maximum allowed value $g_{\omega\rho\pi} = 15.5$ mentioned above. In the latter case, when the inequality (24) is saturated, the quantity I' defined in (23) is zero and the upper and lower bounds written in (22) become equal. Therefore, as shown in Fig. 4, the allowed band of the modulus shrinks in this case to a line. The curves show that the bounds exhibit a monotonous dependence on the value of $g_{\omega\rho\pi}$, the band obtained with $g_{\omega\rho\pi} = 11.5$ being consistent with the allowed domain obtained using as input $f_1(t)$ from the calculation performed in [11,13]. An important conclusion is that the disagreement with the experimental data around 0.6 GeV is preserved even if the coupling $g_{\omega\rho\pi}$ is increased up to its maximum allowed value.

We show also in Fig. 4 the $\omega\pi$ form factor calculated in [8,9] within an effective field approach. It exhibits a more rapid increase and slightly exceeds the highest allowed band shown in Fig. 4 near 0.6 GeV.

V. DISCUSSION AND CONCLUSIONS

Our study has been motivated by the existence of certain discrepancies between the recent calculations [11,12,14] of the $\omega\pi$ electromagnetic transition form factor in the frame of dispersion theory, and the data measured from the $\omega \to \pi^0\gamma^*$ decay around 0.6 GeV. The present work differs from the previous calculations by the different input used above the $\omega\pi$ threshold t_+: while the investigations [11,12] are based on a standard dispersion relation requiring the knowledge of the discontinuity of the form factor along the whole cut, and the work [14] exploits a model-independent integral condition on the modulus, derived from unitarity and perturbative QCD, we have resorted to experimental data obtained from $e^+e^- \to \omega\pi^0$. In order to avoid model-dependent assumptions at higher energies, where data are not available, we have implemented this information in a conservative way, as a weighted integral (5) of the modulus squared. Since we used experimental data above t_+, the results obtained in the present paper are much stronger than those obtained in [14], where only a theoretical inequality on the modulus above t_+ was exploited.

The aim of our study was to test the consistency of the experimental and theoretical information available on the $\omega\pi$ form factor in a parametrization-free approach. We have derived upper and lower bounds on the modulus for $t < t_+$, using as input the discontinuity (2) in its region of validity below the $\omega\pi$ threshold, and the condition (5) on the modulus above the $\omega\pi$ threshold. Mathematically, the problem is of the type considered some time ago for real-analytic functions in [17,18] and generalized recently to analytic functions which are not of real type in [14].

The results are presented in Figs. 2–4, where we show the allowed ranges of the modulus squared (normalized to its value at $t = 0$), defined by the upper and lower bounds calculated in this paper. The curves have been obtained using the expressions (22), where all the input quantities are known. The main theoretical ingredient of the analysis is the partial wave $f_1(t)$ entering the discontinuity (2). Therefore, it was of interest to establish the influence of the parameters entering this quantity on the final results. The amplitude $f_1(t)$ calculated in [12,13] is available in numerical form and its dependence on the free parameters is not very transparent. We have considered therefore the older calculation based on N/D formalism performed in [10], which has the advantage of displaying in an explicit way the dependence on the input parameters, and have improved it by a prescription suggested in [27] for including the effect of rescattering in the crossed channels.

Our study has shown that including the rescattering has the effect of shifting down the allowed band for the modulus of the form factor in the region $t < t_-$. However, in the frame of the N/D model the effect is quite modest, of a few percents. On the other hand, the bounds are quite sensitive to the coupling $g_{\omega\rho\pi}$, which enters as input in the calculation of $f_1(t)$ in the N/D formalism. The results obtained with $f_1(t)$ from [11,13] can be reproduced by using the value $g_{\omega\rho\pi} = 11.5$ in the improved N/D formalism. It turns out that values of $g_{\omega\rho\pi}$ larger than 15.5 are excluded, being inconsistent with the data above t_+ and the value (8) at $t = 0$. By increasing $g_{\omega\rho\pi}$, the allowed bands are pushed upwards. However, as shown in Fig. 4, the narrow band calculated with the maximum allowed value of $g_{\omega\rho\pi}$ is still significantly lower than the experimental data from [5–7] near 0.6 GeV.

Our results indicate a clear conflict between the experimental data on the modulus of the $\omega\pi$ form factor measured in the decay region $t < t_-$ from $\omega \to \pi^0\gamma^*$ and in the scattering region $t > t_+$ from $e^+e^- \to \omega\pi^0$. We note that possible discrepancies between the data on the modulus measured at energies below t_- and above t_+ have been noticed also in the attempts to describe the form factor with specific parametrizations [27]. In contrast, no parametrization of the form factor was necessary in our analysis. The present paper confirms the conclusions of other recent dispersive analyses [11,14] and brings further arguments in support of renewed experimental efforts to measure more precisely the ω conversion decays [37,38].

ACKNOWLEDGMENTS

I would like to thank B. Moussallam for very interesting discussions, and B. Ananthanarayan and B. Kubis for a pleasant collaboration on the work [14] and useful suggestions on the manuscript. This work was supported by UEFISCDI under Contract Idei-PCE No. 121/2011 and by the Ministry of Education and Scientific Research, Romania under Contract PN No. 09370102/2009.

APPENDIX: IMPROVED N/D TREATMENT OF THE $\omega\pi \to \pi\pi$ AMPLITUDE

The N/D model proposed in [10] does not include the rescattering between all the final pions in the kinematical region where the ω decay to three pions is allowed. In this Appendix we briefly describe the model and present a simple modification, which is able to capture the characteristic features of the full solution.

For convenience, we use in this Appendix the notation of [10]. The relation with the conventions used in the text is clear by comparing Eqs. (5.1) and (5.3) of [10] with Eqs. (2) and (4) of this paper, respectively. The P partial wave amplitude of the scattering process (3), denoted in [10] as $t^1(t)$, has dimensions of GeV^{-2} and is related to the partial wave $f_1(t)$ of [11,13] by

$$t^1(t) = \frac{2}{3} m_\omega f_1(t). \tag{A1}$$

In the N/D formalism, the amplitude $t^1(t)$ is written as [10]

$$t^1(t) = t^1_L(t) + t^1_R(t), \tag{A2}$$

where $t^1_L(t)$ has only a left-hand cut and $t^1_R(t)$ has only a right-hand cut for $t > 4m_\pi^2$.

The piece $t^1_L(t)$ was calculated in [10] as

$$t^1_L(t) = \frac{1}{2}\int_{-1}^{1} dz [d^2_{00}(\theta) - d^0_{00}(\theta)] T_{su}(t,z), \tag{A3}$$

where $z \equiv \cos\theta$, $d^j_{m'm}(\theta)$ are elements of Wigner's d-matrix and

$$T_{su}(t,z) = -\frac{4}{3} g_1 g_2 \left(\frac{1}{m_\rho^2 - s(t,z)} + \frac{1}{m_\rho^2 - u(t,z)} \right) \tag{A4}$$

is the ρ-pole contribution in the crossed channels. The dimensionless coupling constants are defined as [10]

$$g_1 \equiv g_{\rho\pi\pi}, \qquad g_2 \equiv g_{\omega\rho\pi} \tag{A5}$$

and the Mandelstam variables have the expressions

$$s(t,z) = R(t) + K(t) z, \qquad u(t,z) = R(t) - K(t) z, \tag{A6}$$

with

$$R(t) = \frac{m_\omega^2 + 3m_\pi^2 - t}{2}, \qquad K(t) = 2q(t)p(t), \tag{A7}$$

where $q(t)$ and $p(t)$ are defined below Eqs. (2) and (4), respectively.

The part $t^1_R(t)$ of the amplitude accounts for the rescattering in the direct channel. In the two-pion approximation, unitarity gives

$$\mathrm{disc}[t^1(t)\Omega^{-1}(t)] = 0, \qquad t \geq 4m_\pi^2, \tag{A8}$$

where $\Omega(t)$ is the Omnès function

$$\Omega(t) = \exp\left[\frac{t}{\pi} \int_{4m_\pi^2}^{\infty} \frac{\delta^1_1(t')}{t'(t'-t)} dt \right], \tag{A9}$$

which is analytic without zeros in the t-plane cut for $t > 4m_\pi^2$ and is normalized to $\Omega(0) = 1$. It can be written above the cut as

$$\Omega(t + i\epsilon) = |\Omega(t)| e^{i\delta^1_1(t)}, \qquad t \geq 4m_\pi^2, \tag{A10}$$

where $\delta^1_1(t)$ is the phase shift of the P wave of the elastic pion-pion amplitude.

Since $t^1_L(t)$ is regular for $t \geq 4m_\pi^2$, from (A2) and (A10) it follows that

$$\mathrm{disc}[t^1_R(t)\Omega^{-1}(t)] = -2i t^1_L(t) \mathrm{Im}[\Omega^{-1}(t)]. \tag{A11}$$

From the discontinuity one can reconstruct the function by means of a standard dispersion relation, written in [10] as

$$t^1_R(t)\Omega^{-1}(t) = a + \frac{t - t_0}{\pi} \int_{4m_\pi^2}^{\infty} \frac{t^1_L(t') \sin\delta^1_1(t')}{|\Omega(t')|(t' - t_0)(t' - t)} dt, \tag{A12}$$

in terms of the unknown subtraction constant a. Combined with (A2), this leads to

$$t^1(t) = \Omega(t) \left[\frac{t^1_L(t)}{\Omega(t)} + a + \frac{t - t_0}{\pi} \int_{4m_\pi^2}^{\infty} \frac{t^1_L(t') \sin\delta^1_1(t')}{|\Omega(t')|(t' - t_0)(t' - t)} dt \right]. \tag{A13}$$

In [10], instead of the Omnès function $\Omega(t)$ a Gounaris-Sakurai parametrization [39] was actually adopted, which is a reasonable approximation on the right-hand cut where it is employed. Thus,

$$\Omega(t) \Rightarrow GS(t) = \frac{D(0)}{D(t)}, \tag{A14}$$

where $D(t)$ is written as

$$D(t) = m_\rho^2 - t - g(t) - i m_\rho \Gamma_\rho(t). \tag{A15}$$

In this relation

$$\Gamma_\rho(t) = \frac{m_\rho}{\sqrt{t}} \left(\frac{q(t)}{q(m_\rho^2)} \right)^3 \Gamma_\rho \tag{A16}$$

is the energy-dependent ρ width defined in terms of the physical width $\Gamma_\rho = 147.8 \pm 0.9$ MeV [32], and

$$g(t) = \frac{m_\rho \Gamma_\rho}{q(m_\rho^2)}(k(t) - k(m_\rho^2) - (t - m_\rho^2)k'(m_\rho^2)),$$
$$k(t) = \frac{2q(t)^3}{\pi\sqrt{t}} \ln \frac{2q(t) + \sqrt{t}}{2m_\pi}. \quad \text{(A17)}$$

Choosing the subtraction point at $t_0 = m_\rho^2$, the behavior of $t^1(t)$ near $t = m_\rho^2$ implies

$$a = \frac{4}{3}\frac{g_1 g_2}{D(0)}. \quad \text{(A18)}$$

Then, the representation (A13) is written finally as [10]

$$t^1(t) = \frac{1}{D(t)}\left[t_L^1(t)D(t) + \frac{4}{3}g_1 g_2 + \frac{m_\rho(t - m_\rho^2)}{\pi}\int_{4m_\pi^2}^{\infty} \frac{t_L^1(t')\Gamma_\rho(t')}{(t' - m_\rho^2)(t' - t)}dt\right]. \quad \text{(A19)}$$

As follows from (A3) and (A4), $t_L^1(t)$ is real for $t > 4m_\pi^2$, which implies that the imaginary terms within the square brackets compensate each other. Therefore, the phase of $t^1(t)$ is equal to the phase of the Omnès function $1/D(t)$, i.e., to the phase shift $\delta_1^1(t)$. In this model, $t^1(t)$ satisfies the Watson theorem, and leads to a purely imaginary discontinuity (2) of the $\omega\pi$ form factor. As shown in [11–13], these properties are no longer valid in the more rigorous treatments of the amplitude.

An obvious shortcoming of the model [10] is the fact that the amplitude $t_L^1(t)$ was calculated in terms of a ρ-meson exchange neglecting the width of the ρ. In this approximation the ω meson is actually stable since its mass is lower that the mass of $\rho\pi$ pair. To improve the model, a straightforward procedure would be to include a finite width for the ρ poles in the denominators of (A4). We have adopted the prescription proposed in [27], where finite-width resonance exchange amplitudes with correct analyticity properties were obtained by replacing

$$\frac{1}{m_\rho^2 - s(t,z)} \Rightarrow \frac{1}{\pi}\int_{4m_\pi^2}^{\infty} dx \frac{\sigma(x)}{x - s(t,z)}, \quad \text{(A20)}$$

and similarly for the u-channel contribution. The pole was replaced by a modified Breit-Wigner expression which automatically ensures the absence of singularities in the complex plane except for a right-hand cut. As suggested in [27], a reasonable choice for the spectral function $\sigma(x)$ is the imaginary part of the Breit-Wigner propagator:

$$\sigma(x) = \frac{m_\rho \Gamma_\rho(x)}{(m_\rho^2 - x)^2 + m_\rho^2(\Gamma_\rho(x))^2}, \quad \text{(A21)}$$

with $\Gamma_\rho(x)$ defined in (A16). In the limit of zero width, $\Gamma_\rho \to 0$, when $\sigma(x) \to \pi\delta(x - m_\rho^2)$, the left side of (A20) is recovered.

By inserting the prescription (A20) in (A3) and (A4), the integration upon $z \equiv \cos\theta$ can be performed exactly, leading to

$$t_L^1(t) = \frac{4g_1 g_2}{3}\frac{1}{\pi}\int_{4m_\pi^2}^{\infty} dx \sigma(x)\frac{F(Z)}{K(t)}, \quad \text{(A22)}$$

where

$$F(y) = \frac{3}{4}\left[2y + (1 - y^2)\ln\frac{y+1}{y-1}\right], \quad \text{(A23)}$$

and

$$Z = \frac{x - R(t)}{K(t)}, \quad \text{(A24)}$$

with $R(t)$ and $K(t)$ defined in (A7).

The singularities of $t_L^1(t)$ in the complex plane arise from the singularities of the function $F(y)$ at $y = \pm 1$ produced by the logarithm, which depend parametrically on x. When x varies along the integration range in (A22), the singularities describe paths in the complex t-plane and in principle can overlap with the t-channel unitarity cut along the real semiaxis $t \geq 4m_\pi^2$. The overlap can be avoided by a suitable prescription. In the present study we have adopted the prescription proposed in [40], which consists in adding to m_ω^2 a small imaginary part, i.e., $m_\omega^2 \to m_\omega^2 + i\epsilon$, with $\epsilon > 0$. With this prescription, we checked numerically that the singularities of $t_L^1(t)$ do not cross the unitarity cut in the t-plane. Moreover, the amplitude $t_L^1(t)$ has no discontinuity across the line $t \geq 4m_\pi^2$, although it is no longer real on the unitarity cut.

The points $t = 4m_\pi^2$ and $t = t_\pm$, i.e., the physical thresholds and the pseudo-threshold t_-, require special attention since there the function $K(t)$ defined in (A7) vanishes. By using the asymptotic expansion

$$F(y) \sim \frac{1}{y} + \frac{1}{5y^3} + \cdots, \qquad |y| \gg 1, \quad \text{(A25)}$$

and the decrease $\sigma(x) \sim 1/x$, we have checked explicitly that in the present model $t_L^1(t)$ is regular at these points.

Since the amplitude $t_L^1(t)$ calculated from (A22) has no discontinuity across the unitarity cut $t \geq 4m_\pi^2$, the representation (A19) remains valid. However, as mentioned above, $t_L^1(t)$ is complex for $t \geq 4m_\pi^2$. Therefore, from (A19) it follows that the phase of the amplitude $t^1(t)$ for $t \geq 4m_\pi^2$ is no longer equal to the phase $\delta_1^1(t)$ of the function $1/D(t)$. Watson theorem, which was valid in the original N/D model, is no longer valid now. Moreover, the amplitude is not an analytic function of real type. These properties are satisfied of course by the exact solution $f_1(t)$ calculated in [11–13].

It is useful to compare the simple improved N/D model presented here with the exact amplitude calculated by solving numerically integral equations of the Khuri-Treiman type. An obvious feature of the N/D model is the lack of symmetry between the direct (t) and the crossed (s and u) channels. In fact, in the decay region the dynamics in the three two-pion channels must be the same. In the Khuri-Treiman formalism, by iteratively solving the relevant integral equation, the symmetry between the three channels is gradually increased. This adjustment is not performed in the N/D approach, which has a rigid structure. However, by improving the description of the crossed channels in the frame of the N/D model, the main features of the exact partial wave amplitude $f_1(t)$, namely the failure of Watson theorem and the breakdown of the reality property, appear in a natural way.

[1] E. Czerwiński *et al.*, MesonNet workshop on meson transition form factors, arXiv:1207.6556.

[2] G. Colangelo, M. Hoferichter, B. Kubis, M. Procura, and P. Stoffer, Towards a data-driven analysis of hadronic light-by-light scattering, Phys. Lett. B **738**, 6 (2014).

[3] F. Jegerlehner and A. Nyffeler, The muon g-2, Phys. Rep. **477**, 1 (2009).

[4] M. Benayoun *et al.*, Hadronic contributions to the muon anomalous magnetic moment workshop. $(g-2)_\mu$: Quo vadis? workshop. Mini proceedings, arXiv:1407.4021.

[5] R. I. Dzhelyadin *et al.*, Study of the electromagnetic transition form-factor in $\omega \to \pi^0\mu^+\mu^-$ decay, Phys. Lett. **102B**, 296 (1981).

[6] R. Arnaldi *et al.* (NA60 Collaboration), Study of the electromagnetic transition form-factors in $\eta \to \mu^+\mu^-\gamma$ and $\omega \to \mu^+\mu^-\pi^0$ decays with NA60, Phys. Lett. B **677**, 260 (2009).

[7] G. Usai (NA60 Collaboration), Low mass dimuon production in proton-nucleus collisions at 400 GeV/c, Nucl. Phys. **A855**, 189 (2011).

[8] C. Terschlüsen and S. Leupold, Electromagnetic transition form factors of light vector mesons, Phys. Lett. B **691**, 191 (2010).

[9] C. Terschlüsen, S. Leupold, and M. F. M. Lutz, Electromagnetic transitions in an effective chiral Lagrangian with the η' and light vector mesons, Eur. Phys. J. A **48**, 190 (2012).

[10] G. Köpp, Dispersion calculation of the transition form-factor $F_{\pi\omega\gamma}(t)$ with cut contributions, Phys. Rev. D **10**, 932 (1974).

[11] S. P. Schneider, B. Kubis, and F. Niecknig, The $\omega \to \pi^0\gamma^*$ and $\phi \to \pi^0\gamma^*$ transition form factors in dispersion theory, Phys. Rev. D **86**, 054013 (2012).

[12] I. V. Danilkin, C. Fernández-Ramírez, P. Guo, V. Mathieu, D. Schott, M. Shi, and A. P. Szczepaniak, Dispersive analysis of $\omega/\phi \to 3\pi, \pi\gamma^*$, Phys. Rev. D **91**, 094029 (2015).

[13] F. Niecknig, B. Kubis, and S. P. Schneider, Dispersive analysis of $\omega \to 3\pi$ and $\phi \to 3\pi$ decays, Eur. Phys. J. C **72**, 2014 (2012).

[14] B. Ananthanarayan, I. Caprini, and B. Kubis, Constraints on the $\omega\pi$ form factor from analyticity and unitarity, Eur. Phys. J. C **74**, 3209 (2014).

[15] S. Okubo, Exact bounds for K_{l3} decay parameters, Phys. Rev. D **3**, 2807 (1971).

[16] G. Abbas, B. Ananthanarayan, I. Caprini, I. Sentitemsu Imsong, and S. Ramanan, Theory of unitarity bounds and low energy form factors, Eur. Phys. J. A **45**, 389 (2010).

[17] I. Caprini, Constraints on physical amplitudes derived from a modified analytic interpolation problem, J. Phys. A **14**, 1271 (1981).

[18] I. Caprini, I. Guiasu, and E. E. Radescu, Model independent dispersion approach to proton Compton scattering, Phys. Rev. D **25**, 1808 (1982).

[19] S. I. Dolinsky *et al.*, The reaction $e^+e^- \to \omega\pi^0$ in the center-of-mass energy range from 1.0 GeV to 1.4 GeV, Phys. Lett. B **174**, 453 (1986).

[20] D. Bisello *et al.* (DM2 Collaboration), e^+e^- annihilation into multihadrons in the 1350–2400 MeV energy range, Nucl. Phys. B, Proc. Suppl. **21**, 111 (1991).

[21] M. N. Achasov *et al.* (SND Collaboration), The process $e^+e^- \to \omega\pi^0 \to \pi^0\pi^0\gamma$ up to 1.4 GeV, Phys. Lett. B **486**, 29 (2000).

[22] R. R. Akhmetshin *et al.* (CMD-2 Collaboration), Study of the process $e^+e^- \to \omega\pi^0 \to \pi^0\pi^0\gamma$ in c.m. energy range 920–1380 MeV at CMD-2, Phys. Lett. B **562**, 173 (2003).

[23] M. N. Achasov *et al.*, Measurement of the cross section for the $e^+e^- \to \omega\pi^0 \to \pi^0\pi^0\gamma$ process in the energy range of 1.1–1.9 GeV, JETP Lett. **94**, 734 (2012).

[24] K. W. Edwards *et al.* (CLEO Collaboration), Resonant structure of $\tau \to 3\pi\pi^0\nu_\tau$ and $\tau \to \omega\pi\nu_\tau$ decays, Phys. Rev. D **61**, 072003 (2000).

[25] F. Ambrosino *et al.* (KLOE Collaboration), Study of the process $e^+e^- \to \omega\pi^0$ in the ϕ-meson mass region with the KLOE detector, Phys. Lett. B **669**, 223 (2008).

[26] N. N. Khuri and S. B. Treiman, Pion-pion scattering and $K^\pm \to 3\pi$ decay, Phys. Rev. **119**, 1115 (1960).

[27] B. Moussallam, Unified dispersive approach to real and virtual photon-photon scattering at low energy, Eur. Phys. J. C **73**, 2539 (2013).

[28] K. M. Watson, Some general relations between the photoproduction and scattering of π mesons, Phys. Rev. **95**, 228 (1954).

[29] G. P. Lepage and S. J. Brodsky, Exclusive processes in quantum chromodynamics: Evolution equations for hadronic wave functions and the form-factors of mesons, Phys. Lett. B **87**, 359 (1979).

[30] B. Ananthanarayan, I. Caprini, D. Das, and I. S. Imsong, Parametrization-free determination of the shape parameters

for the pion electromagnetic form factor, Eur. Phys. J. C **73**, 2520 (2013).
[31] B. Ananthanarayan, I. Caprini, D. Das, and I. S. Imsong, Two-pion low-energy contribution to the muon $g-2$ with improved precision from analyticity and unitarity, Phys. Rev. D **89**, 036007 (2014).
[32] K. A. Olive *et al.* (Particle Data Group Collaboration), Review of particle physics, Chin. Phys. C **38**, 090001 (2014).
[33] P. L. Duren, *Theory of H^p Spaces* (Academic Press, New York, 1970).
[34] R. Omnès, On the solution of certain singular integral equations of quantum field theory, Nuovo Cimento **8**, 316 (1958).
[35] R. García-Martín, R. Kamiński, J. R. Peláez, J. Ruiz de Elvira, and F. J. Ynduráin, The pion-pion scattering amplitude. IV: Improved analysis with once subtracted Roy-like equations up to 1100 MeV, Phys. Rev. D **83**, 074004 (2011).
[36] I. Caprini, G. Colangelo, and H. Leutwyler, Regge analysis of the $\pi\pi$ scattering amplitude, Eur. Phys. J. C **72**, 1860 (2012).
[37] F. A. Khan (WASA-at-COSY Collaboration), in *Proceedings of the second International PrimeNet Workshop*, edited by P. Adlarson *et al.*, arXiv:1204.5509.
[38] M. J. Amaryan (CLAS Collaboration), in *MesonNet 2013 International Workshop. Mini-proceedings*, edited by K. Kampf *et al.*, arXiv:1308.2575.
[39] G. J. Gounaris and J. J. Sakurai, Finite Width Corrections to the Vector Meson Dominance Prediction for $\rho \to e^+e^-$, Phys. Rev. Lett. **21**, 244 (1968).
[40] J. B. Bronzan and C. Kacser, Khuri-Treiman representation and perturbation theory, Phys. Rev. **132**, 2703 (1963).